

A standardized modeling system for assaying tau toxicity in *Drosophila melanogaster*

Margaret Houston

Submitted in Partial Fulfillment of the Requirements for Graduation

from the Malone University Honors Program

Adviser: Kathryn Huisinga, Ph. D.

April 19, 2017

1

**Abstract**

Recent Alzheimer's studies have shown conflicting results about the toxicity of tau protein, the major constituent of neurofibrillary tangles and a hallmark of Alzheimer's disease, in *Drosophila melanogaster* fruit fly models. Current research has used rough eye phenotypes and random transgene insertion to model this phenomenon in flies with varied indications of toxicity. This project is the first phase of a multi-year study that aims to better understand and standardize methods for tau modeling in flies. These

standardization methods include controlling the location of transgene insertion using  $\phi$ C31 technology and exploring new readout methods such as sensory bristles. We believe that measuring toxicity using sensory bristles may be more sensitive than in the eyes and can be more easily quantified for comparison in experiments. Thus far, we have prepared the tau transgene for insertion into live flies and begun collection of baseline data for normal fly eyes and number of sensory bristles.

## **Background**

As of 2017, an estimated 5.5 million Americans are living with Alzheimer's Disease (AD), a debilitating neurodegenerative disease largely associated with aging<sup>1</sup>. With recent advances in medicine and the aging baby boomer generation, the 65 and older demographic is projected to encompass 20 percent of the total U.S. population by the year 2030<sup>2</sup> and roughly double from 48 million to 88 million by the year 2050<sup>1</sup> (Figure 1).

As this elderly population continues to increase, so does the incidence of AD. Currently, one in ten individuals over the age of 65 is living with Alzheimer’s dementia . Despite the increased focus on Alzheimer’s research, it is still the sixth leading cause of death in America<sup>3</sup> and the only one that cannot be prevented, slowed, or cured<sup>1</sup>.

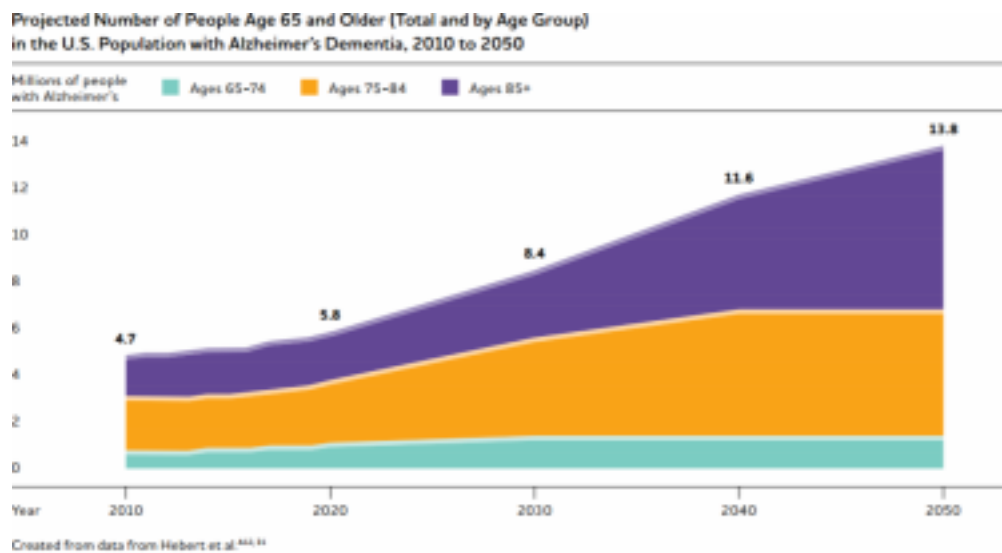


**Figure 1.** Projected increase in AD prevalence by 2050<sup>1</sup>.

Alzheimer’s disease is more than just America’s problem—it is a global issue. Nearly 44 million people in the world are living with AD or a related dementia, yet only one in

four affected individuals is aware of their diagnosis or receiving treatment.

3

Globally, the cost of Alzheimer's and dementia is estimated to be \$605 billion, approximately 1% of the global gross domestic product<sup>4</sup>.

The pathology of Alzheimer's disease is attributed to two key proteins: amyloid  $\beta$ , a 42 amino acid fragment ( $A\beta$  42) of the amyloid precursor protein (APP) and tau protein. These proteins have been implicated in the formation of AD's pathological hallmarks: the accumulation of amyloid plaques, enriched in  $A\beta$ 42, and neurofibrillary tangles (NFT), enriched in tau<sup>5</sup>. Amyloid plaques accumulate *outside* neurons and interfere with synaptic communication while NFTs form *inside* neurons and interfere with movement of nutrients and other essential molecules (Figure 2). According to the current understanding of AD pathology, amyloid plaques and NFTs have two separate pathologies, but they are related to one another as NFT formation occurs downstream of plaque formation. Together, these elements contribute to cell death. Initially, the brain is able to compensate for the dead neurons and AD symptoms may go unnoticed for many

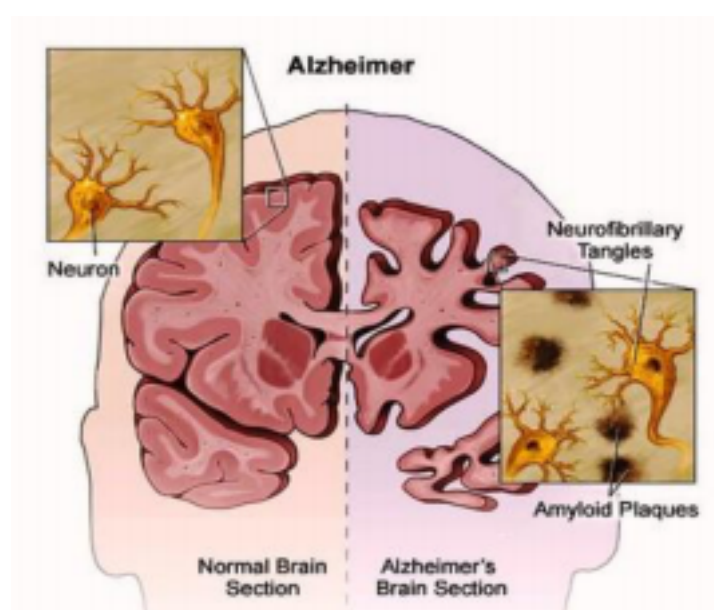


**Figure 2.** Pathology of AD, roles of plaques and NFTs in brain degeneration<sup>6</sup>

4

years. In the later stages, however, so many neurons die that the brain can no longer compensate and mental decline becomes apparent<sup>1</sup>. Eventually, individuals sustain enough damage that they require assistance for even simple daily tasks such as getting out of bed, dressing, eating and bathing. This disease places a large burden on the

families of affected individuals as well as the nation's nursing homes and assisted living facilities<sup>2</sup>. To combat this growing problem, we must learn more about how AD progresses, and most importantly, learn how to slow this progression.

The current understanding of AD pathology is that tau works downstream of A $\beta$ 42 and promotes neuronal toxicity and death<sup>5</sup>. APP is a type I integral membrane protein involved in vesicle transport in axons as well as regulating signaling across the synaptic space. There are many known APP mutations that lead to early onset, familial AD that cause its long, extracellular domain to be cleaved by  $\gamma$ -secretases producing the toxic A $\beta$ 42 fragment commonly found in amyloid plaques. In addition, APP also has protective function and is upregulated after brain trauma and appears to have similar activity in cases of progressive neurodegeneration<sup>7</sup>.

Accumulation of the A $\beta$ 42 fragment cleaved from APP has been demonstrated to aggregate between neurons and disrupt synaptic activity, causing loss of memory and rhythmic behaviors. This toxicity may also be due in part to the mislocalization of mitochondria from the axons to cell bodies, causing stress on the endoplasmic reticulum and autophagy. The main foci of research for these proteins are the mechanisms of initiation and toxicity as well as pharmacological suppression of A $\beta$ 42 toxicity<sup>7</sup>.

Tau protein, found predominantly in axons of mature neurons, is highly soluble, natively unfolded, and phosphorylated at multiple sites. Its structure (Figure 3) contains

5

two domains: an N-terminal projection domain with up to two N-terminal repeated sequences (N) and a proline rich region; and a microtubule binding domain with up to four 31 amino acid carboxy-terminal tandem repeat sequences (R). In humans, tau has

six isoforms that arise from alternative splicing of the MAPT gene and contain varying numbers of N (0N, 1N, 2N) and R (3R, 4R) repeats. The expression of each isoform is tissue specific and the protein plays integral roles in embryogenesis and early development<sup>9</sup>. While tau has various isoforms, most of its diversity stems from posttranslational-modifications including O-glycosylation, ubiquitination, sumoylation, nitration, glycation, acetylation, cross linking by transglutaminase, isomerization, conformational changes, phosphorylation, and proteolytic cleavage<sup>7</sup>. These posttranslational modifications are considered key to tau's toxicity because there is no known causative mutation identified in tau protein.

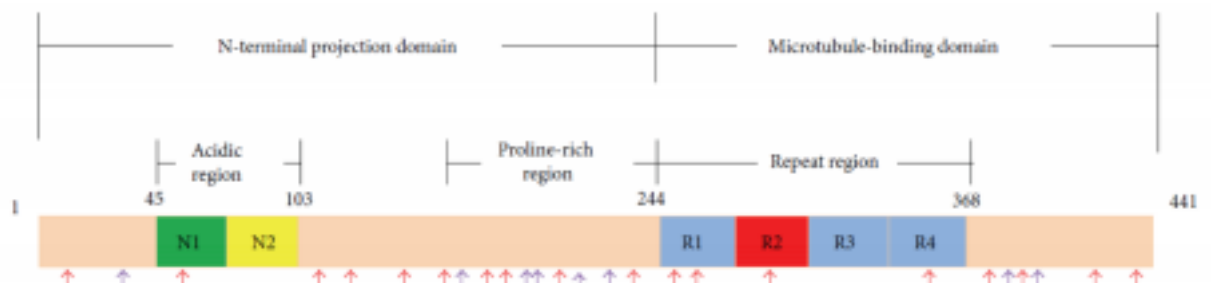


**Figure 3.** Structure of human tau protein<sup>8</sup>

Phosphorylation of tau has profound effects on its affinity for microtubules (Figure 4). Hypophosphorylation increases affinity, while hyperphosphorylation decreases affinity thus destabilizing microtubule network. Hyperphosphorylated tau is the major constituent in the neurofibrillary tangles characteristically found in AD<sup>10</sup>. Tau

phosphorylation, therefore, has become one of the major focuses of recent research. In addition to its effects on microtubule affinity, phosphorylation of tau is also thought to

6

affect its susceptibility to cleavage. The calcium dependent, cysteine protease, calpain is known to cleave tau and is thought to be responsible for fragments that greatly contribute to tau's toxicity in the context of AD<sup>11</sup>.

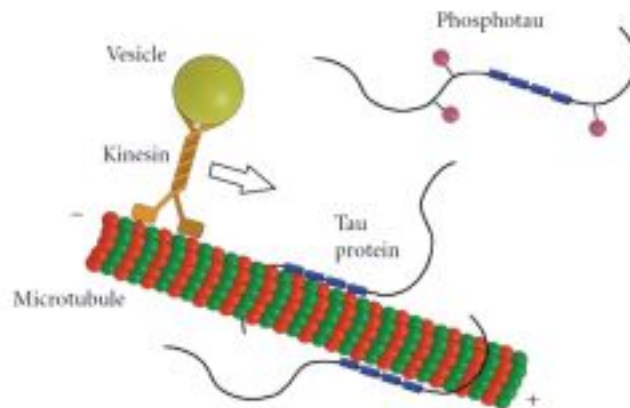


**Figure 4.** Native tau protein and interaction with microtubules<sup>9</sup>

The majority of researchers in this area use the fruit fly, *Drosophila melanogaster*, as a model for tau toxicity because of its short generation time, ease of screening, and



sequenced genome. For these studies, human tau protein is inserted into the fly genome and expressed using the GAL4-UAS system (Figure 5). This system consists of the yeast GAL4 transcriptional activator and a transgene controlled by an

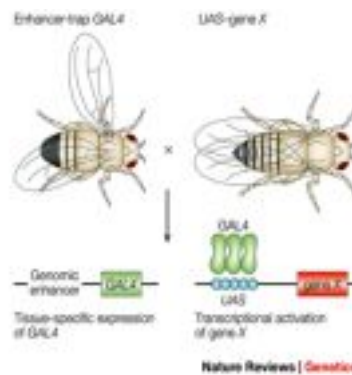


**Figure 5.** GAL4-UAS system and its application to tissue-specific expression<sup>12</sup>.

7

upstream activating sequence (UAS) promoter that is inactive in the absence of GAL4. The GAL4-UAS system is generally used in genetic overexpression and tissue-specific genetic mutant rescue<sup>13</sup>.

Specific drivers are used to express a transgene only in a certain tissue. The GMR driver is most frequently used in tau toxicity studies because it causes expression in the eyes which is most convenient for screening. This works with the GAL4-UAS system as follows: the *glass* transcription factor in the eye induces the expression of GAL4 in all of

the eye cells from the larval stage—this is the fly line containing the GMR driver. The cDNA for a human disease-associated gene (such as that of tau protein) is subcloned into a UAS expression construct, creating a line of transgenic flies. When the driver line and the transgenic line are crossed, the expression of the human gene in their progeny is regulated by the presence of GAL4 which is only found in the cells of the eyes. Therefore, the human gene is only expressed in the eyes and nowhere else in the fly<sup>14</sup>. Normally, the *Drosophila* eye has 800 highly regularly spaced ommatidia containing 8 photoreceptor neurons<sup>10</sup>. The human gene's level of toxicity is measured using a qualitative determination of “roughness” to the eyes ranging from subtle to severe. These designations are based on examining the angles and distances between ommatidial centers as well as changes in eye color, shape, size, bristles or texture<sup>15</sup>. While this is an effective method for quick and easy assessment of toxicity and making general comparisons, this method lacks the sensitivity to differentiate between mutant toxicities that produce similar phenotypes. In addition, it can be challenging to make comparisons between studies as the classifications of phenotypes can be relatively subjective (Figure 6). In this way, it is also more difficult to recognize subtle pattern formation. It is of note that one lab has recently developed an

8

automated system for the assessment of eye phenotypes, but the cost and availability of this technology is still unknown<sup>15</sup>.

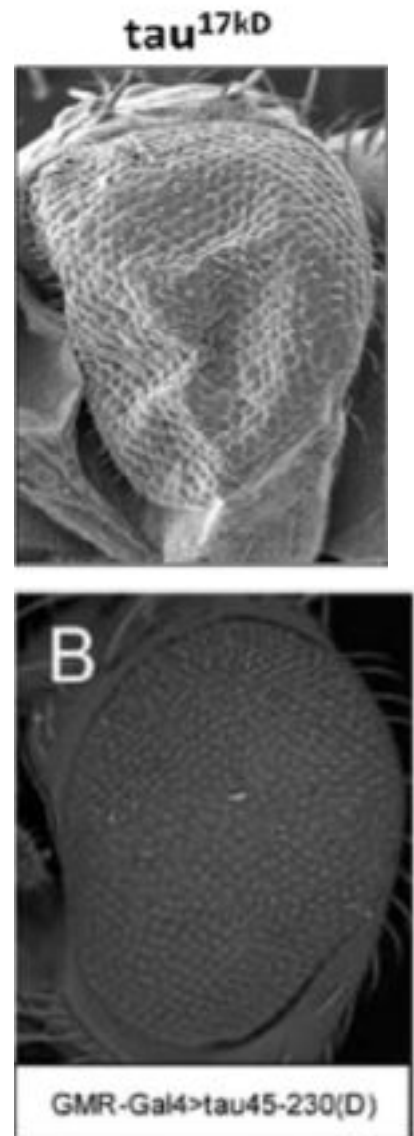


**Figure 6.** Shows the various results obtained in similar studies. From Reinecke pictured on left<sup>11</sup>, Geng pictured on right<sup>16</sup>. Both show the expression of the 17kD tau fragment.

A study by Yeh and colleagues suggested a better, less ambiguous method of screening. Rather than expressing a transgene in the eyes, they express it in the notum using the Eq driver. This driver works with the same GAL4-UAS system described previously, but the Eq driver expresses GAL4 in the sensory bristles located on the fly's back (notum). On

average, flies have approximately 200 notal bristles that can be lost due to neurodegeneration, making it a good tool to assay tau toxicity<sup>17</sup>(Figure 7). Utilizing the notum bristle patterns, while more work intensive as far as counting individual hairs, enables the standardization of values and quantification of toxicity<sup>17</sup>. Ideally, the ability to objectively quantify results will increase overall sensitivity and could highlight the minute differences between various forms of tau. If this method proves to be effective, it

9

will be much easier to compile and search through a database of quantities than to look at various pictures that are chosen at the discretion of each individual lab. This issue is demonstrated when comparing the photos of tau toxicity between articles by Geng and Reinecke (Figure 6)—they show the same genes, but one looks more severely affected than the other. Creating a database that contains the results of previous toxicity experiments would create more unity in the field by compiling and condensing the findings we have thus far, allowing us to get a sense of the bigger picture.

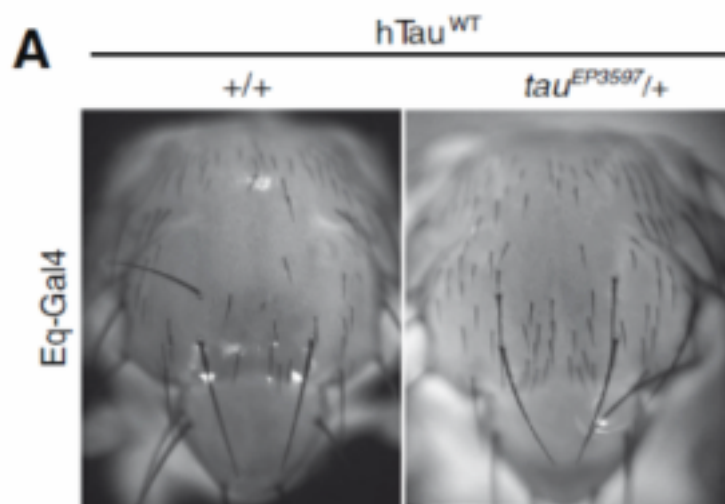


**Figure 7.** Expression of transgene toxicity using notal bristles<sup>17</sup>.

In flies, transgene expression and modifications can be affected to some degree by locational variability. For example, if a gene is randomly inserted into an area of a chromosome that is not easily accessible to translation proteins, the gene may be expressed at low levels or not at all. On the other hand, a gene could be expressed at very

high levels if it is placed in a location that is easily accessible. This variability in expression is particularly problematic in toxicity studies because it becomes difficult to

10

distinguish whether the signs of toxicity are due to the manipulation of variables or the effect of positional variation. By examining the effects when transgenes placed in consistent locations, this variability is eliminated and the results are directly comparable<sup>18</sup>. This lends a higher degree of consistency to results. If this methodology were adopted by researchers in this field, it would be possible compare a wide array of tau variations. In 2013, Povellato and colleagues developed several novel fly strains to potentially address the issue of positional variability. They developed five fly strains that expressed tau in a unique, constant location in the genome. The insertion sites utilized were 51C, 68A, 68C, 86F, and 96E. The technology used to achieve this positional constancy is called  $\phi$ C31 integrase which uses a serine integrase from the bacteriophage  $\phi$ C31. This integrase facilitates a sequence-directed recombination between a bacterial attachment site (attB) in the plasmid containing the transgene and a pseudo phage attachment site (pseudo attP) found in the fly genome allowing to the precise insertion of the gene into the target genome within the sequence of the attP site<sup>19</sup> (Figure 8). When using this technology, the position of the transgene within the UAS construct is controlled by the placement of these landing sites. When crossed with a specific driver line (GMR or Eq), the progeny will express the transgene only in the desired region and maintain positional consistency through generations ensuring the same levels of genetic accessibility and levels of expression. In doing this, Povellato and colleagues were able to assess the levels of tau expression at each position and directly compare the toxicity of different tau mutations that aim to alter the protein's interactions. This control is

invaluable in developing the consistency in results necessary to make informed

11

conclusions about factors such as phosphorylation or proteolytic cleavage that can affect tau toxicity in a living system.

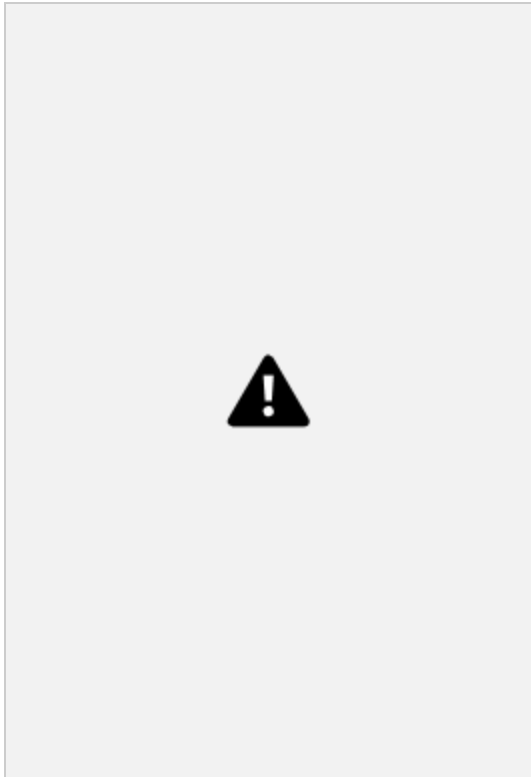
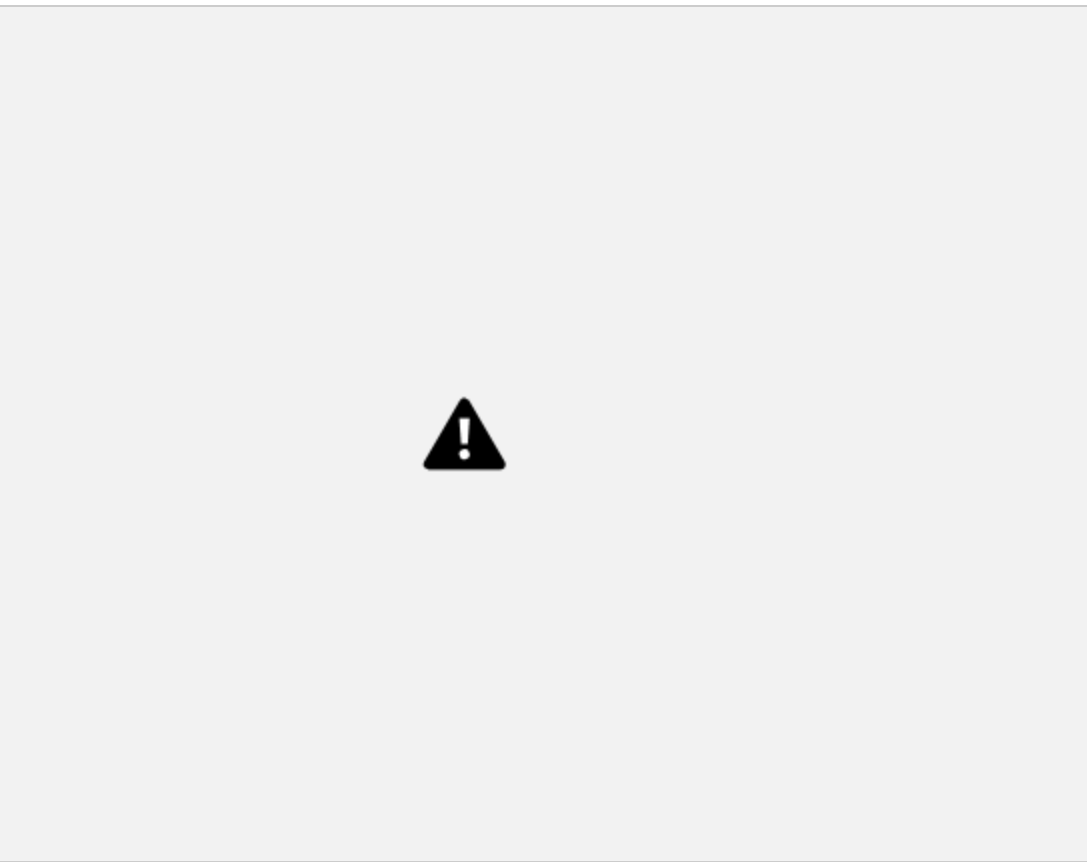


**Figure 8.** Insertion of a transgene into a target genome using  $\phi$ C31 integrase<sup>19</sup>.



## **Materials and Methods**

### Preparation of tau DNA construct

The genetic material encoding the full length-human tau protein was amplified from the tau/pET29b (Figure 9), a DH5 $\alpha$  bacterial vector, a gift from Peter Klein (Addgene plasmid # 16316)<sup>21</sup> The plasmid was streaked on LB plates with kanamycin and incubated at 37°C overnight. Several isolated colonies were transferred to LB liquid cultures containing kanamycin, where they were incubated for an additional 16 hours with shaking. The bacterial cells were harvested by centrifuging at 13,000 rpm.



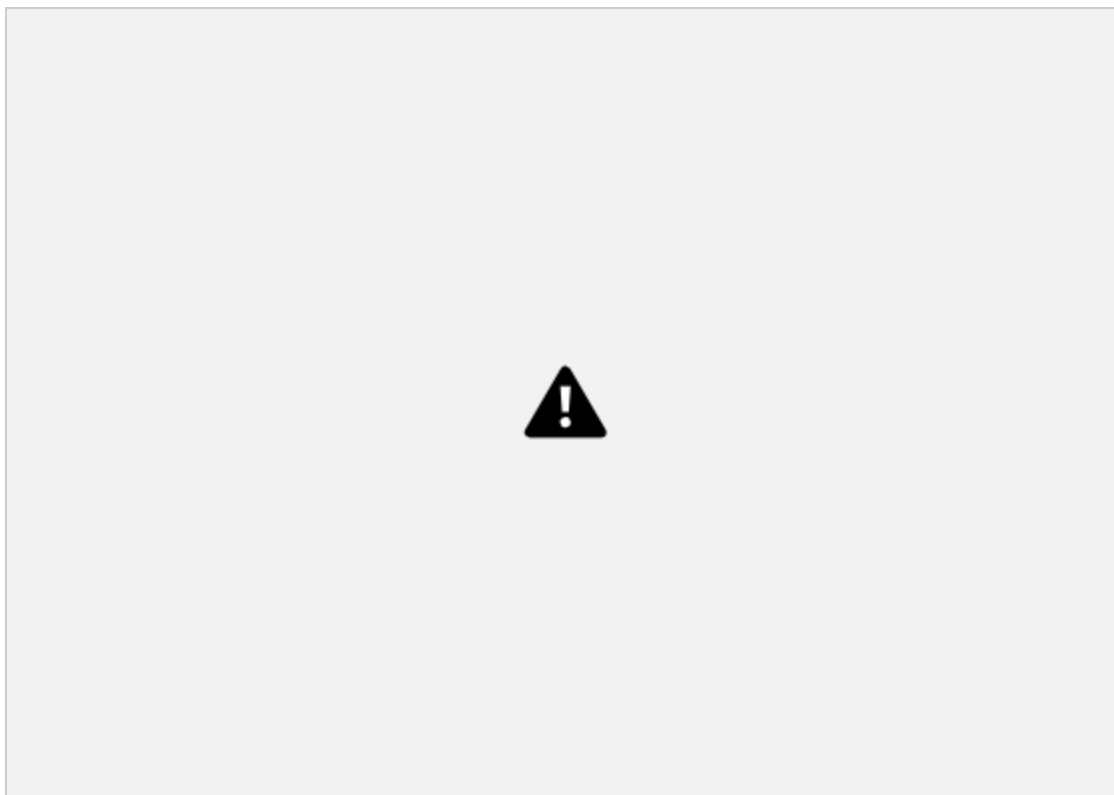


**Figure 9.** Tau/pET29b bacterial vector<sup>21</sup>.

The tau/pET29b DNA was obtained from the pelleted *E. coli* using a QIAprep Miniprep kit (Qiagen). The procedure was performed in accordance with the

13  
manufacturer's instructions. The plasmid DNA in the column was eluted from the QIAprep spin column with 50  $\mu$ L Buffer EB.

The concentration of plasmid DNA was determined in a SPECTROstar<sup>Nano</sup> using an LVis plate. Absorption of DNA at 260nm was used to determine concentration. Restriction enzyme digest was used to confirm the structure of the plasmid (Figure 10). A master mix containing 0.3 U/ $\mu$ L SacI, 1x NEB Cutsmart buffer, 1x BSA, distilled water was used to digest a series of 1  $\mu$ g samples of plasmid DNA.



**Figure 10.** Diagram of LR *in vitro* recombination<sup>22</sup>.

Samples were run on a standard 1% agarose gel containing ethidium bromide.

Loading buffer was added in appropriate proportions to each sample and placed in wells. Gels were run at 105 V for 30-35 minutes. Bands were then visualized by UV light and photographs were taken using the Gel Logic 100 Imaging System.

14

PCR primers were designed according to the specifications in the pENTR Directional Cloning Kit manual from Invitrogen. Primers were designed to amplify the sequence of tau in the pET29b plasmid. The primer sequences were as follows: 5' primer: 5'-

CAC CAT GGC TGA GCC CCA GGA-3'

3' primer: 5'-ACC GGT TCG TCC CAA ACA CT-3'

The PCR mixture contained .5 uM forward and reverse primers, 200 uM dNTPs, and 0.02 U/ $\mu$ L Q5 High Fidelity DNA polymerase from NEB, and 1x Q5 reaction buffer supplied with the DNA polymerase. The reactions were performed with several template concentrations to ensure optimal results. The reactions were placed in the thermocycler at 98°C for 30 seconds, then underwent 30 cycles of 98°C for 10 seconds, 71°C for 30 seconds, and 72°C for 45 seconds. This was followed by a 10-minute final extension period at 72°C. The PCR products were removed promptly and stored at 4°C. The PCR products were confirmed with gel electrophoresis.

Invitrogen's pENTR/D-TOPO Cloning Kit was used for high efficiency transformation of tau into chemically competent *E. coli*. The 3' single stranded overhang added to the tau DNA sequence during PCR was complementary to the overhang in the cloning vector allowing for the directional joining of the double-stranded DNA with the correct orientation<sup>23</sup>. PCR product was roughly quantified using gel electrophoresis to ensure the optimal PCR product: vector molar ratio (between 0.5:1 and 2:1). The TOPO cloning

reaction contained fresh PCR product, salt solution (12 M NaCl, 0.06 M MgCl<sub>2</sub>), sterile water, and the TOPO vector. Four separate TOPO reactions were used: two with varied volumes of PCR product, a control PCR product (ligation control), and a vector only control. This reaction mixture was used to transform One Shot<sup>®</sup> Competent *E. coli*.

15

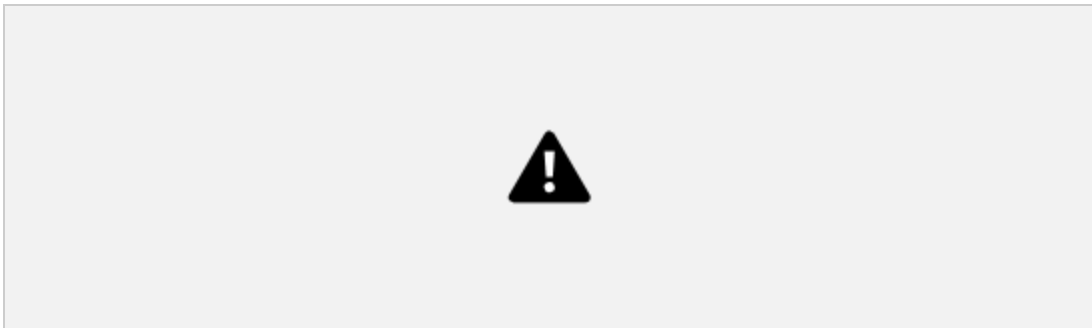
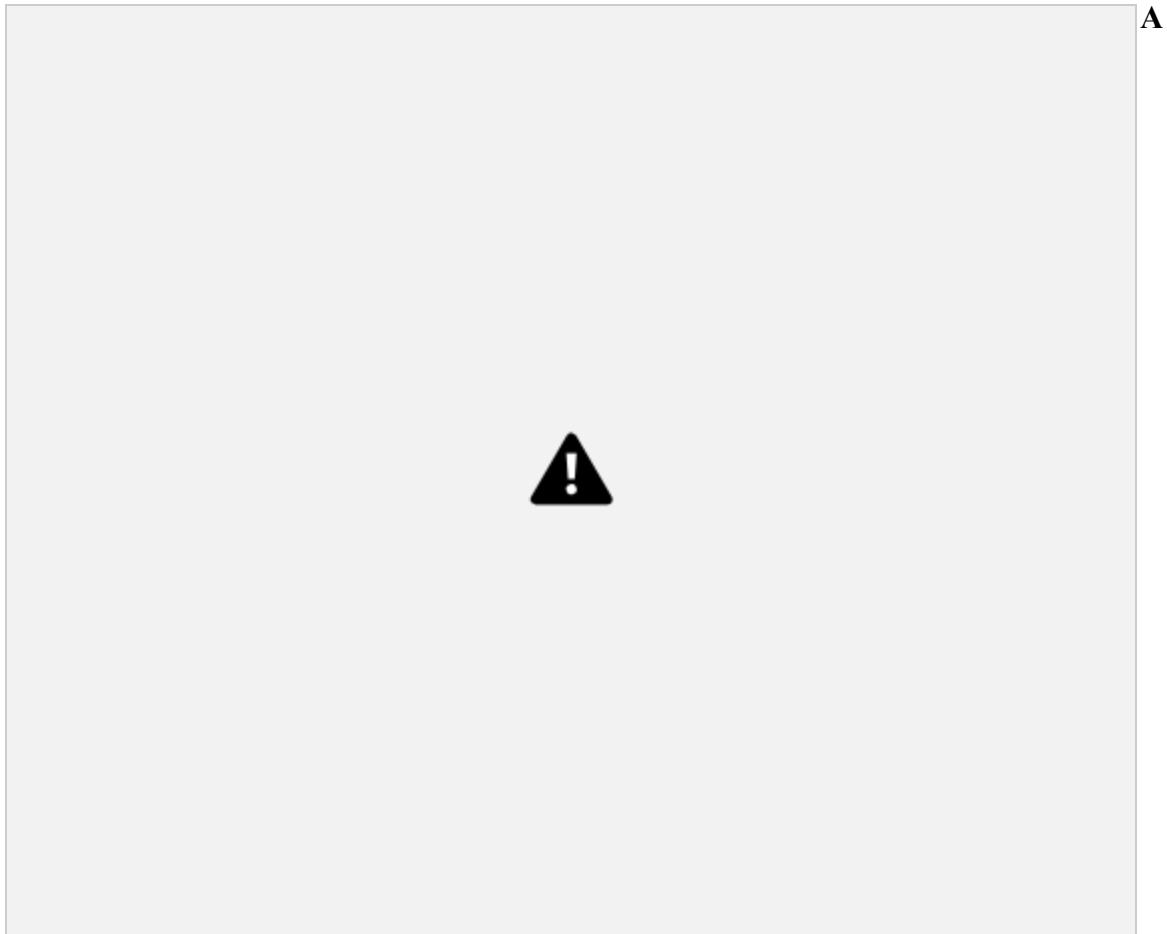
Transformations of the four TOPO reactions and a pUC19 transformation control were performed to manufacturer specifications. The transformed *E. coli* were grown in SOC media and two different volumes of each TOPO reaction were spread on kanamycin plates. Plates containing ampicillin were used for the pUC19 control.

Preparing the tau construct in the entry clone for transformation into the destination vector entailed similar procedure to that described previously. *E. coli* containing the entry clone were grown in overnight LB liquid cultures with kanamycin and pelleted. The QIAprep Miniprep kit (Qiagen) was used to prepare tau DNA with LR recombination sites. The procedure was performed in accordance with the manufacturer's instructions. The plasmid DNA in the column was eluted from the QIAprep spin column nm on a Lvis plate in the SPECTROstar<sup>Nano</sup>. A double restriction enzyme digest with SacI and NotI was performed to confirm the structure of the entry clone. A master mix containing 0.5 U/μL of SacI and NotI, 1x NEB Cutsmart buffer, and distilled water. Samples were then run on a standard agarose gel as described previously. Establishing Fly Lines

Though the tau construct is not yet complete, fly strains containing the GMR and Eq drivers were crossed with flies containing the φC31 landing site at chromosomal position 68A. All strains were obtained from Bloomington Drosophila Stock Center.

Figure 11 contains relevant information about each line and crosses performed.

16



**B**



**Figure 11. A.** Diagram of cross between flies containing Eq driver and 68A landing pad site. **B.** Diagram of cross between flies containing GMR driver and 68A landing pad. These crosses serve as controls that do not contain the tau insert.

#### Preparation of Destination Vector

The vector pTW from the Drosophila Gateway™ Vector collection was recommended for GAL4- driven somatic expression *in vivo* without N-terminal or C terminal tags. This destination vector is designed to recombine with the tau entry clone to produce an expression clone that can be placed into the fly to develop a new strain (Figure 10). The plasmid was streaked on LB plates with chloramphenicol and incubated at 37°C overnight then transferred to chloramphenicol LB liquid cultures. The bacteria were pelleted and the vector DNA was obtained using a QIAprep Miniprep kit (Qiagen). The procedure was performed in accordance with the manufacturer's instructions. The

17

DNA in the column was eluted from the QIAprep spin column with 50 µL Buffer EB and confirmed using standard gel electrophoresis.

**Results & Discussion**

Preparation of tau DNA construct



The first step of the experiment for examining Tau in flies is to create a plasmid that can be inserted into their genome. This entails growing and amplifying the human tau gene from a bacterial plasmid. The initial streaking of the tau/pET29b plasmid produced fair levels of growth with good colony spacing. After incubation, liquid cultures appeared moderately dense. Despite promising appearance, LVis data collected suggested very low DNA yields (Table 1), despite tau/pET29b being a high-copy plasmid. The miniprep kit and reagents were examined to ensure there were no missing or damaged reagents. New liquid cultures were produced from the same plate, but showed even less growth with an extended incubation period (21 hours). Of five cultures, only two showed reasonable growth, two showed low growth, and one showed none. New plates were streaked and the process was repeated. Liquid culture growth improved, but LVis results continued to indicate low DNA concentrations (Table 1). Because PCR requires only a small sample of DNA, the samples from the minipreps were pooled for an enzyme digest.

**11/17/16 12/6/16**

**Sample # Concentration (ng/uL)**

<sup>1</sup> 82.3225 35.325

<sup>2</sup> 20.8225 25.480

<sup>3</sup> 14.8425 34.245

<sup>4</sup> 45.4675 19.290

**Table 1.** Concentration of tau/pET29b plasmid DNA after miniprep.

The purpose of the enzyme digest is to confirm that the DNA in the sample is the gene of interest. Specific enzymes will make cuts at specific sequence patterns. The identity of the gene can be confirmed when enzyme cuts match those that are expected based on the map. A digest was performed with SacI, but provided poorly visible bands. A subsequent digest was completed from the same sample with larger DNA quantities and additional enzymes, HindIII and BamHI (Figure 12, Figure 13). This also proved ineffective due to incorrect proportions in the digest mixture. A final digest was performed with SacI and BamHI, again adjusting proportions to optimize reaction. Another plasmid that was cut by BamHI was used as a control to ensure there was no issue with the enzymes themselves. This digest provided favorable results.



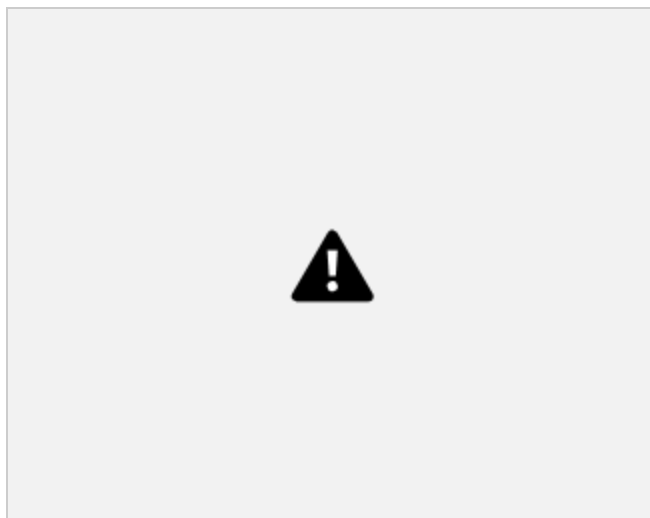


**Figure 12.** Map of BamHI, SacI, and HindIII cutting sites for tau/pET29b plasmid shown in light blue.



**Figure 13.** Enzyme digest results with BamHI, SacI, and HindIII. BamHI digest was expected to linearize tau/Pet29b (6,742 bases). The resulting band appears at approximately 6.7 kB. The SacI digest was expected to yield bands at 5513 bases and 1229 bases. The band that was visualized moved only slightly further than the linearized plasmid at 6.7 kB, suggesting that the SacI enzyme did not successfully cut the plasmid. The HindIII digest was expected to yield bands at 6279 and 463 bases. The placement of the top band appears around 6 kB and the bottom band could not be visualized. Because the smaller end of the ladder is only minimally visible, it may be that a cut was made successfully but the smaller band cannot be seen.



**Figure 14.** The bands on this gel each appear in the expected locations, confirming the presence of tau in the pET29b plasmid.

The first PCR (Figure 15) worked well, but was stored longer than the recommended two-week time frame necessary for the pENTR/D-TOPO reaction to occur without degradation of the entering DNA. A second PCR was performed using the same materials and concentrations but showed no amplification upon analysis. A third was performed using the same protocol, assuming that the previous issue was due to human error. Analysis revealed bands for only the highest and lowest template concentrations (Figure 16). After subsequent procedures, it was determined that incomplete melting of reagents led to inconsistent distribution of reaction components, preventing consistent

22

amplification. The procedure was adjusted appropriately to produce a successful amplification (Figure 17).

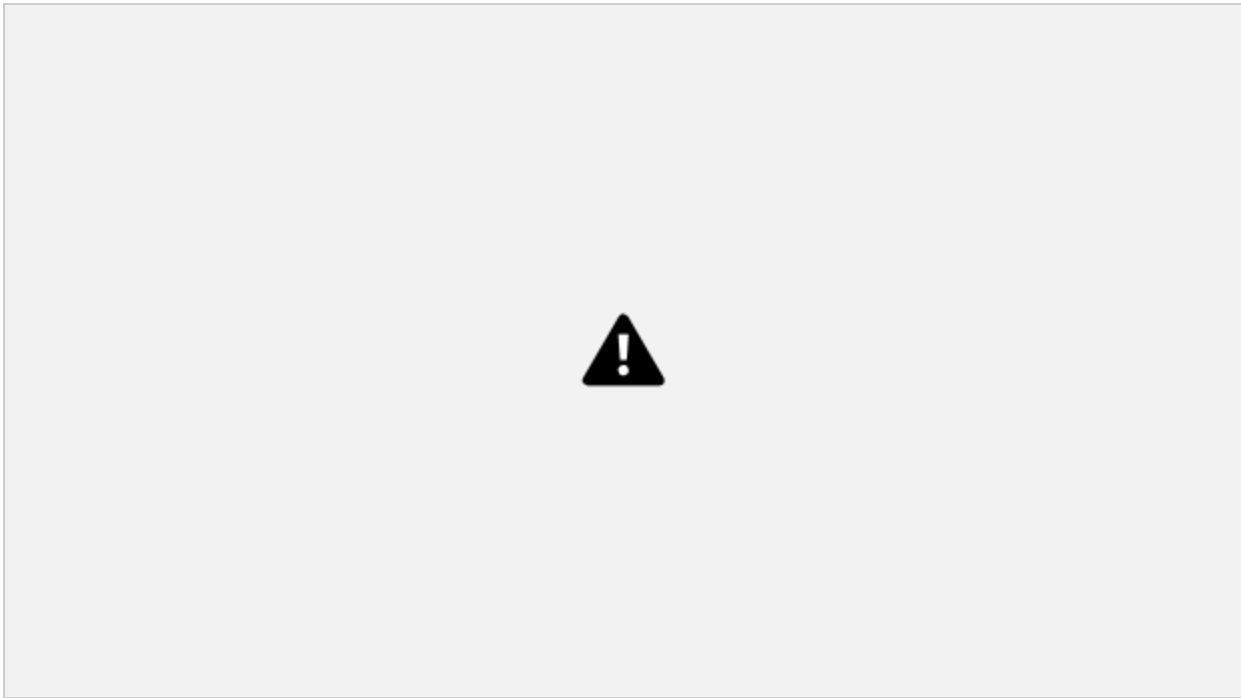


**Figure 15.** Results from the first successful PCR. Bands visualized at 1.4 kB confirming the successful amplification of the tau insert from the plasmid DNA.





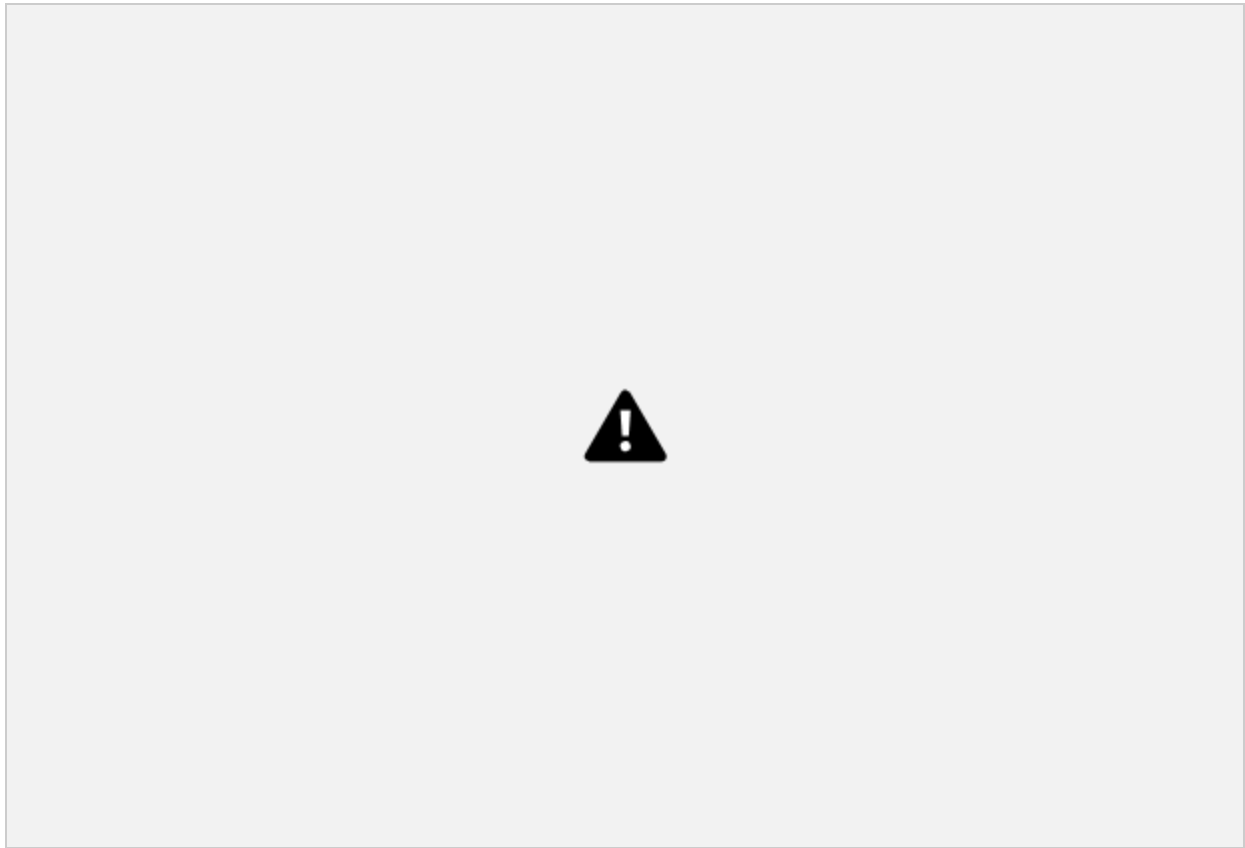


**Figure 16.** This gel shows evidence of inconsistent reagent distribution among samples. Bands are seen clearly at 200 and 0.2 pg/ $\mu$ L and faintly at 2 pg/ $\mu$ L. A successful PCR would have displayed bands in each well with band intensity decreasing relative to concentration.

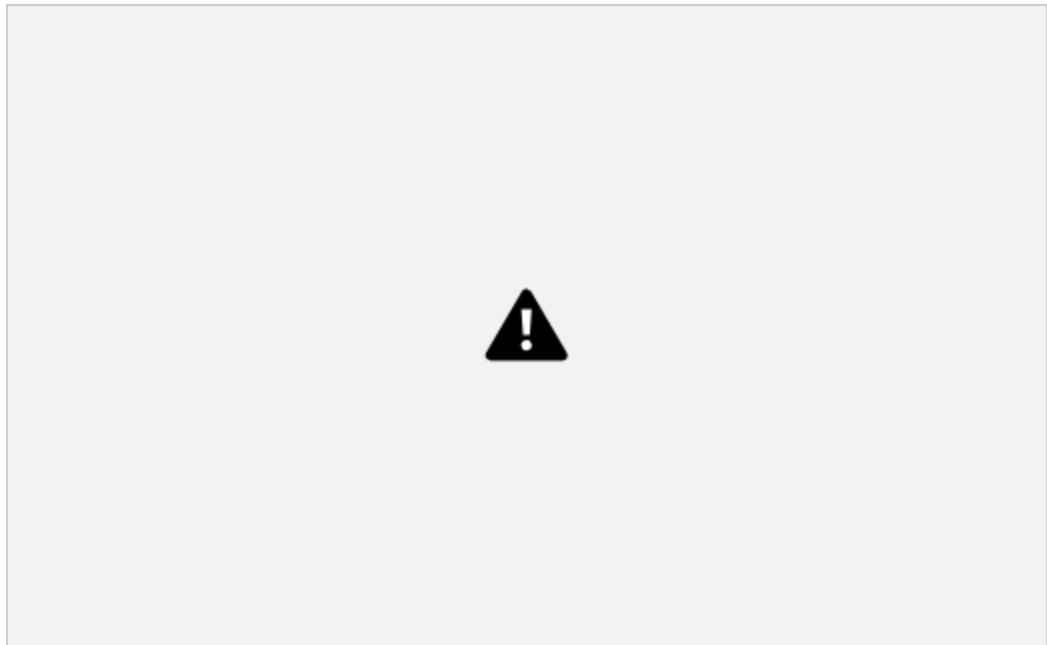
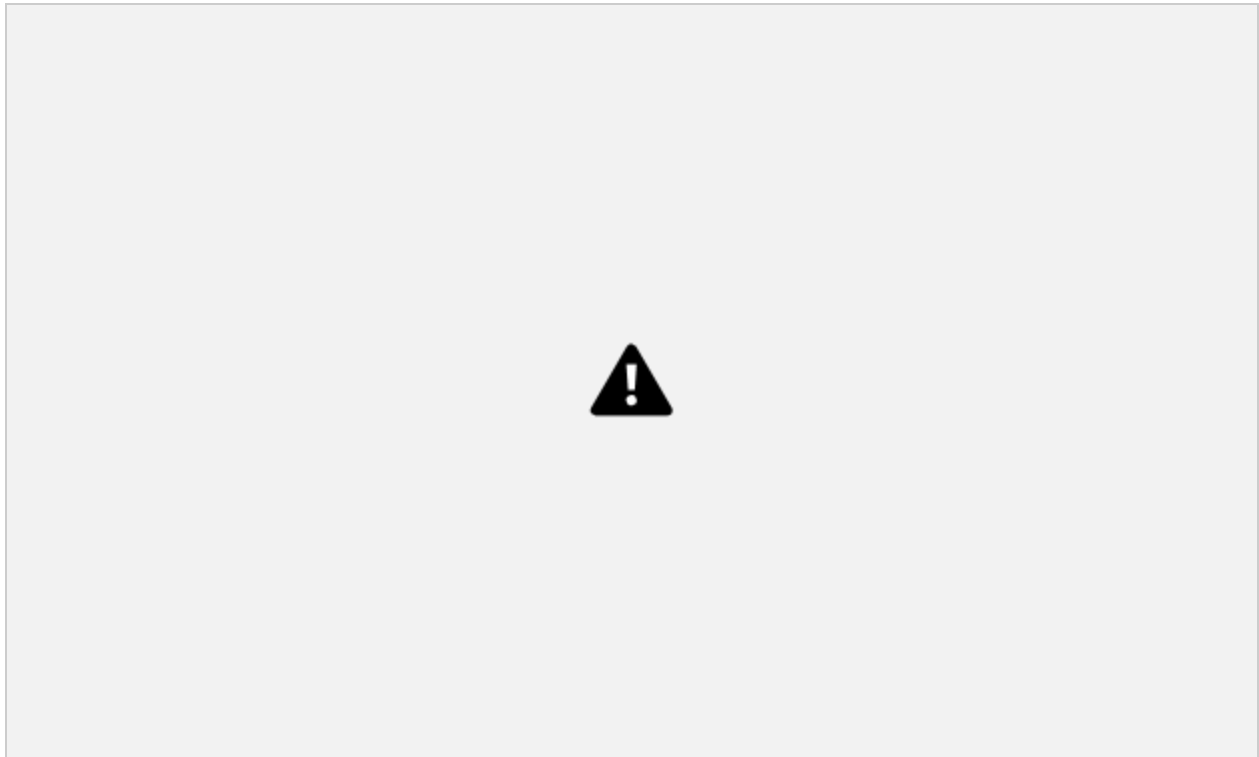


**Figure 17.** Successful PCR samples used for pENTR/D-TOPO cloning. Bands are visualized at 1.4 kB, confirming amplification of tau

places the attL and attR sites on the correct ends of the tau DNA sample and prepares it for entry into the Gateway System. This is the first step to correctly placing the human tau gene into the 68A position in the fly genome using  $\phi$ C31 technology. After the preparation of the entry vector, an expression construct is created by performing an LR recombination with the pTW destination vector. This expression construct is then introduced into the fly genome to express the human tau protein. The pENTR/D-TOPO process utilizes Topoisomerase I from the *Vaccinia* virus cleaves the phosphodiester bond in the DNA backbone, a tyrosyl residue from the topoisomerase binds to the 3' end of the cleaved DNA, and bases are added directionally using the CACC overhang that was added to the forward PCR primer<sup>23</sup>. The initial pENTR/D-TOPO transformation did not produce colonies for any of the TOPO reactions. There were 280 colonies from 0.3 pg of the pUC19 control. The transformation efficiency of  $3.3 \times 10^7$  colony units per ug, roughly 100-fold less than the manufacturer's expected efficiency. This suggested that there was an issue with the cells provided in the kit. Fresh PCR products were obtained and the transformation was repeated. The second transformation was also done according to the manufacturer's protocol. Changes made included new plates with fresh antibiotic and doubling the number of cells plated to increase the potential for viable colonies. In this reaction, the four TOPO reactions and pUC19 control produced no colonies. A third transformation was performed by the thesis adviser and, again, no colonies were produced.

To assess the viability of the One Shot<sup>®</sup> Competent *E. coli* a series of reactions were performed with transformation cells provided by the kit and a pUC plasmid and

the kit were each transformed into the One Shot<sup>®</sup> Competent *E. coli* and DH5 $\alpha$  cells. The results confirmed suspicions concerning the viability of the One Shot<sup>®</sup> cells. The reactions with the lower efficiency DH5 $\alpha$  cells provided colonies, while the One Shot<sup>®</sup> cells showed no growth.

The manufacturer was contacted and new cells were received. Their transformation efficiency was confirmed by the pUC19 control provided in the kit (Figure 18). The same four TOPO reactions were set and successfully produced colonies

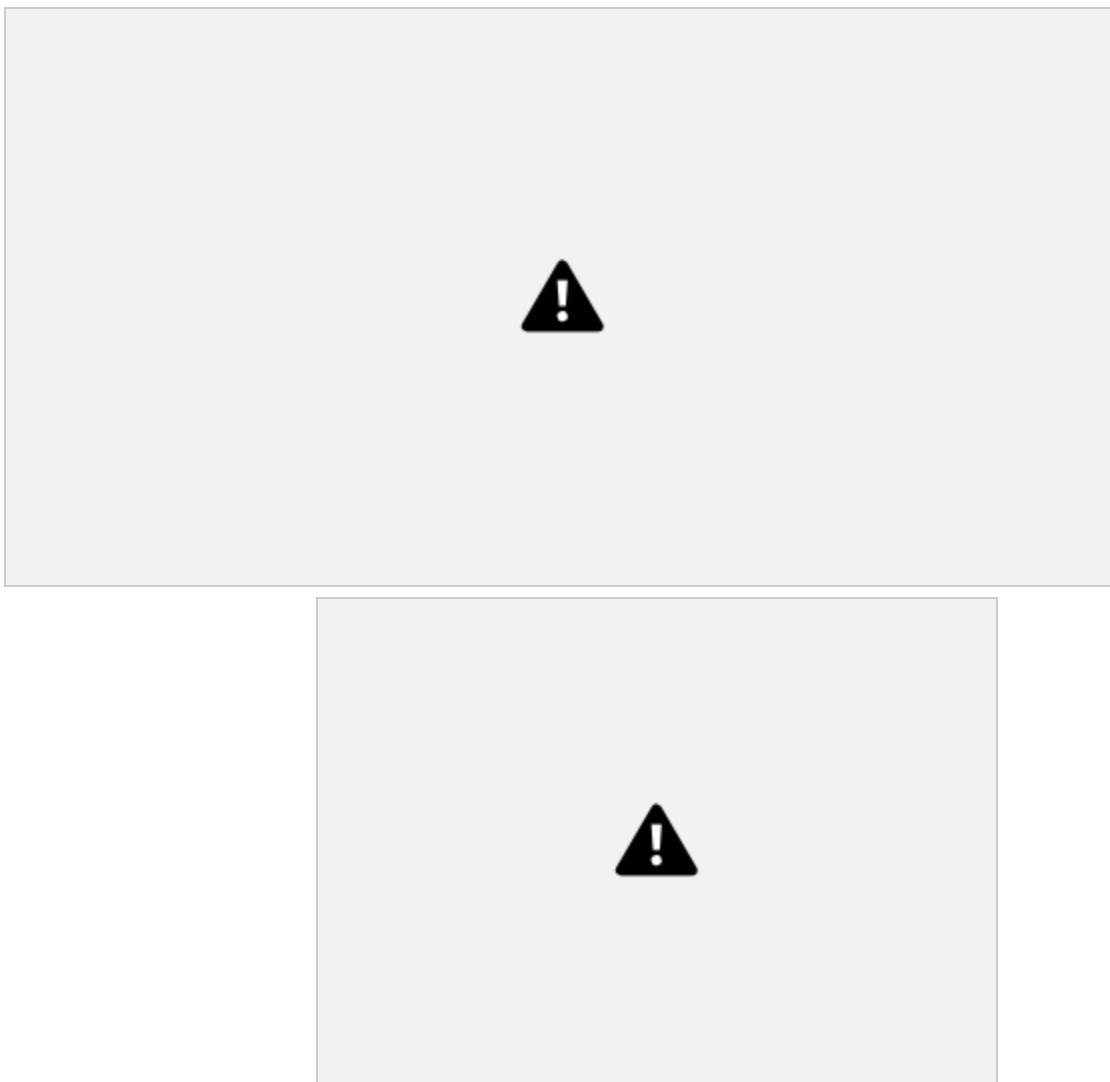


**Figure 18.** Successful pUC19 controls, 200  $\mu$ L plated volume (left), 10  $\mu$ L plated with 20  $\mu$ L SOC (right).

(Table 2) that were minimally visible upon removal from 37°C incubator. The plates were left to continue growth at room temperature for several days. The number of colonies remained the same but became larger and darker compared to control colonies.

26

Number of Colonies

1  $\mu$ L tau template; 100  $\mu$ L plating volume 3

1  $\mu$ L tau template; 200  $\mu$ L plating volume 5

3  $\mu$ L tau template; 100  $\mu$ L plating volume 0

3  $\mu$ L tau template; 200  $\mu$ L plating volume 1

**Table 2.** TOPO transformation products containing tau.

Growth of the pENTR/D-TOPO + tau insert liquid cultures were significantly better than that of the tau/pET29b plasmid. Each culture demonstrated good growth in a shorter period of time. This may have been due in part to the larger size of the initial colonies. After undergoing minipreps, these samples showed a much greater spread in DNA concentrations ranging from approximately 30 ng/ $\mu$ L to 630 ng/ $\mu$ L. This variety may be due in part to the differing densities of each culture.

Analysis of the first enzyme digest attempt showed strong uncut bands, while the cut bands were not visualized or faint. The bands from the digest showed indications of being linearized (bands visible at 3.9 kB), suggesting that either SacI or NotI is not

cutting properly (Figure 19). To address the faintness of the bands, the amount of DNA used in the digest was increased. Similar results were achieved for the second digest.

Samples that underwent digest appeared either to be linearized or uncut with some variation in migration due to supercoil relaxation that occurred over the incubation period. For the third digest, the reaction size and enzyme concentrations were increased to optimize enzyme activity in hopes that both cuts would be clearly visible. In addition to the double digest, samples were individually digested with SacI and NotI to discern which enzyme was not working properly. The results suggested an increase in enzyme

27

activity as more samples were seen with two distinct bands. Assessing the migration of these bands, however, is somewhat problematic. Because all of the band sizes are so close (3.9 kB (linear), 2.8 kB (NotI  $\square$  SacI cut), 2.5 kB (no insert), and various degrees of nicked and uncut in between), it is hard to discern which band belongs to which condition (Figure 20). The single enzyme digests suggested that NotI is either not cutting or the map created for the clone is incorrect and there is no longer a NotI site present in the sequence. This also means that it cannot be reasonably concluded that tau is or is not present in the correct orientation in the entry clone.

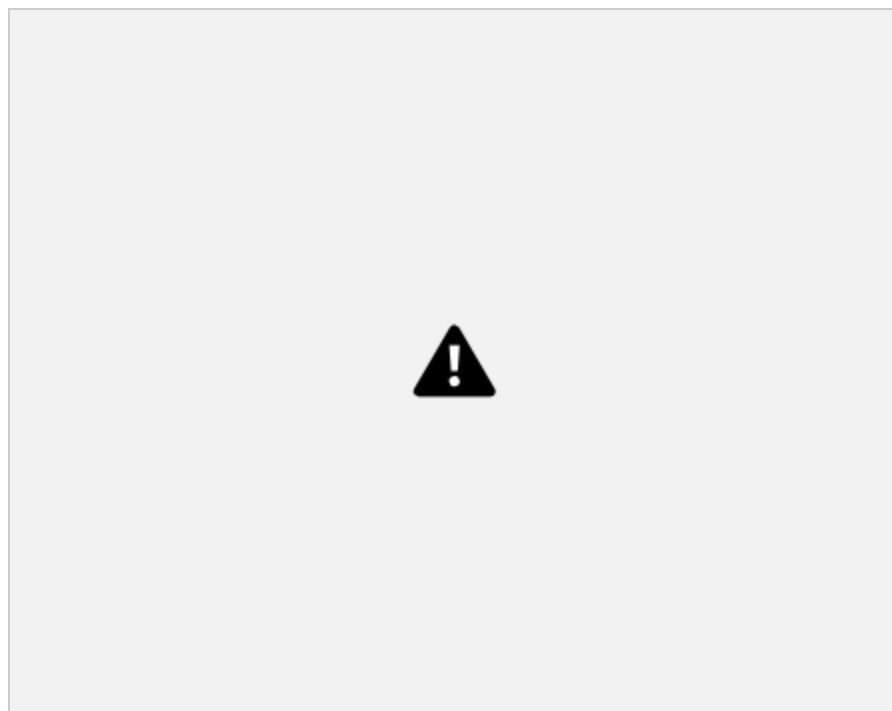
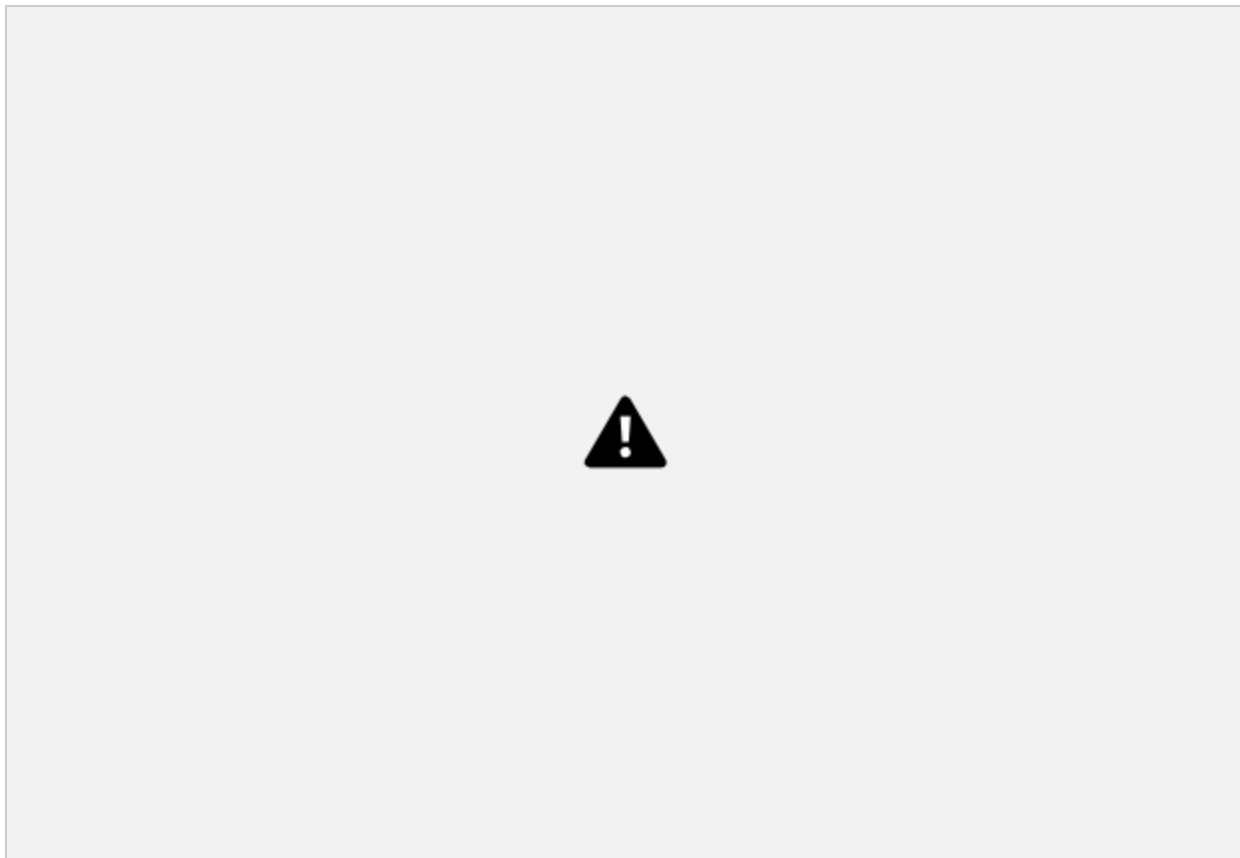


**Figure 19.** Map of pENTR D-TOPO + tau insert. The tau insert is labeled in gray. SacI and NotI digest sites are labeled in light blue. Bands are expected to appear at 1,091 and 2,815 bases as the result of a double digest.





**Figure 20.** This gel shows digest results for replicate tau/pENTR plasmid samples. The

variations between samples suggest inconsistent cutting patterns that include nicks, variation in supercoiling, and incomplete cuts. The samples showing two bands are in the expected areas, but because the single digests should not show two bands, it cannot be reasonably concluded that the insert is present and in the correct orientation. SacI however shows distinct, single bands in the at 3.9 kB which suggest that it has linearized the plasmid. The cutting issue is more likely due to the NotI enzyme, which means that it also cannot be concluded that the tau insert is *not* correct.

### Establishing Fly Lines

Both GMR lines have developed successfully (Figure 21). There has been difficulty in setting Eq crosses due to abnormal timing of eclosion of the line carrying the Eq driver and rarity of virgins. A cross has been successfully set, but no adult progeny have been obtained as of yet.

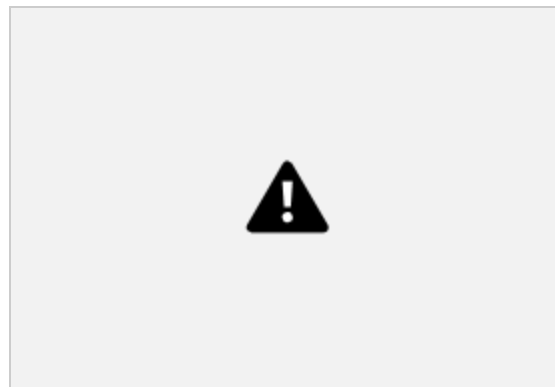
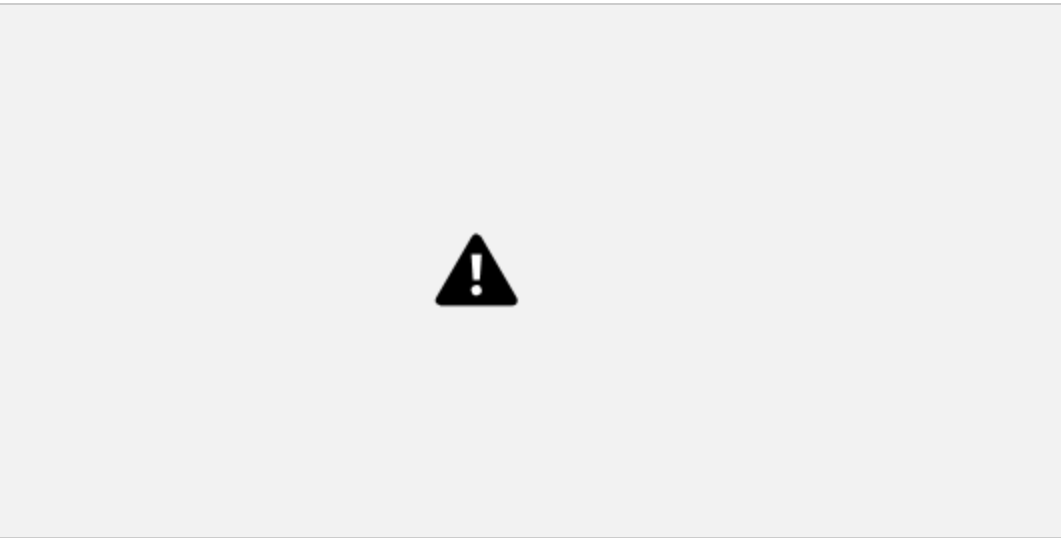


**Figure 21.** Photograph of the GMR-68A control cross shows regularly spaced ommitidial centers, consistent color and texture, and shows no signs of degeneration as a result of the driver or landing pad.

### Preparation of Destination Vector

The destination vector was successfully isolated and the pTW structure was

confirmed by HindIII enzyme digest and analysis by gel electrophoresis (Figure 22).

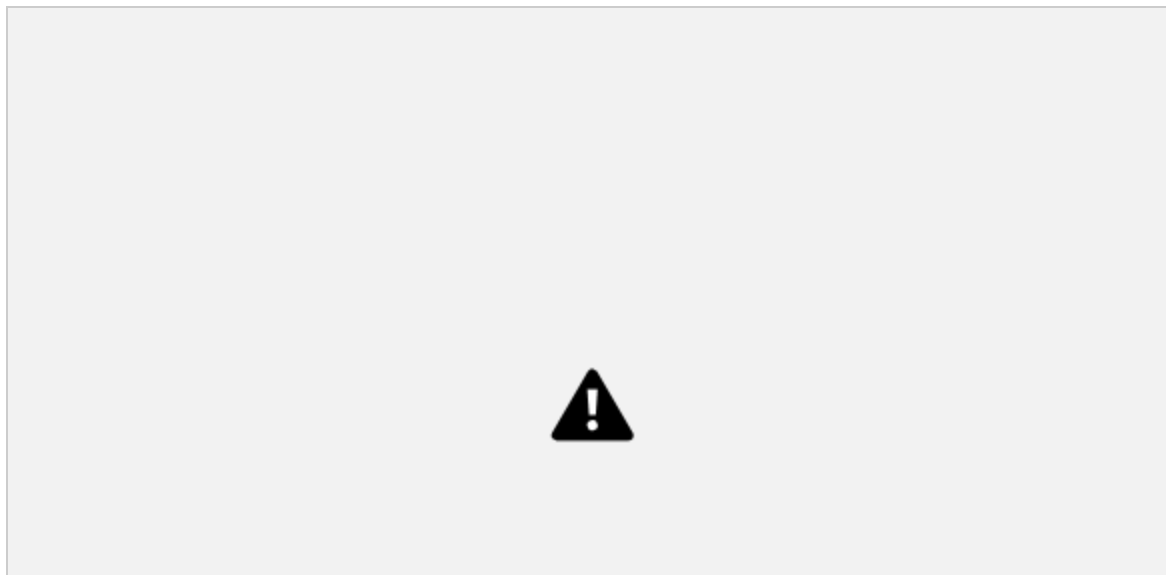




**Figure 22.** Successful preparation of pTW vector. Cuts (C lanes) were made with HindIII with bands expected at 7,360; 3,078; 408; and 24 bp. Only the 7,360 and 3,078 (faintly) are visible on the gel.

### Reflection

The initial experimental plan is much larger than the scope of what was actually achieved over the course of this year. Toxicity of the tau protein can arise from phenomena including proteolytic cleavage. Previous studies have paid significant attention to the 17kD proteolytic tau fragment which is believed to be a toxic resultant from cleavage by the calcium-dependent protease, calpain<sup>5,11</sup>. Recent studies using the model organism, *Drosophila melanogaster* found significantly different results from tau toxicity *in vivo* that may be due to the varied locations of the transgenes within the fly genome<sup>18</sup>. The larger study aims to reconcile these differences by controlling the location of transgene insertion using  $\phi$ C31 technology<sup>19</sup>. Additionally, tau studies involving calpain have only used the rough eye phenotype to assay toxicity. At a later point, study intends to assess tau expression in the notal bristles which has been reported more

sensitive than the current method<sup>17</sup> and presents an opportunity to objectively quantify toxicity by tracking bristle loss. Together eliminating of positional effects and quantifying tau toxicity could provide a means of uniformly standardizing assessment techniques and bringing unity to the field.

While  $\phi$ C31 technology has been used in various tau studies, this project is novel in two respects. First, the few tau studies that have utilized notal expression did not control the location of transgene expression, so site-specific integrases have never been utilized in this context. Secondly, this technology has only been used to examine toxicity due to phosphorylation. This study is unique in utilizing  $\phi$ C31 technology to observe the effects of toxicity due to tau truncation. The precise role of calpain and its contribution to tau toxicity is still unclear due to the disagreements of previous studies. This study aims

31

to address the possible causes of these discrepancies. If these methods are effective, it will allow researchers to make better and more accurate conclusions about calpain's role in the progression of Alzheimer's disease and can be applied to a wider range of toxicity studies to truly make an impact on this line of research.

The overarching plan is to create fly strains expressing the following transgenes of human tau protein would be produced and incorporated into a UAS vector and expressed using both a GMR-Gal4 driver for expression in the eyes and an Eq-Gal4 driver for expression in the notum: tau<sup>WT</sup> (wild-type tau), tau<sup>CR</sup> ("calpain resistant", K44Q/R230Q)<sup>18</sup>, and tau<sup>L43A/V29A</sup>. The mutations in the latter two outline the 17kD fragment. These transgenes will be placed at landing site 68 A using  $\phi$ C31 site directed integrase technology<sup>18,19</sup>. Results would be measured using ommittidial disruption<sup>15</sup> of the

eyes or loss of sensory bristles in the notum, survivorship studies, RNA transcript levels, and quantitative western blot. The survivorship assay will examine the ability of the flies to survive with tau expressed via each driver to examine differences in long term toxicity. The value of each expression method would be determined based on sensitivity to tau<sup>WT</sup>. These results will then be used to determine the relative rescue in toxicity caused by the protective mutations made in tau<sup>CR</sup> and tau<sup>L43A/V29A</sup>.

Looking at what I had planned to do and what I accomplished, I cannot help but feel at least partially disappointed that the experiments did not go more smoothly. I am still unsure that I successfully completed most of the first step outlined in the experimental plan, which falls short of even my “worst-case scenario” expectations. Though things did not turn out as planned experimentally, I would be remiss to ignore the

32

valuable lessons learned about experimental science, unmet expectations, and perseverance from both a scientific and a Christian perspective.

In my experience, I found experimental science to be more difficult than I expected. There is so much that goes into planning experiments. Choosing elements such as the specific fly lines and plasmids took a lot of research. It felt like detective work tracking down the specifics of each component and figuring out what would best suit the needs of the experiment. I learned how to navigate so many data bases that I never knew existed! Having to critically think through every single step and detail of each experiment made me realize how most undergraduate science students take for granted the reagents that are already gathered and procedures that are clearly written with helpful reminders of

what to do or not do at each step. It takes a lot of time and practice to be able to do procedures well and develop genuinely good lab technique (and maintain it when no longer under direct supervision). There are many instances where simply “following the directions” does not cut it. I found it was so important to pay attention to the details of everything I did because sometimes valuable parts of instruction go unwritten. It takes intimate knowledge of the principles behind each procedure to be able to perform tasks well.

For my entire life I have worked hard, gotten good grades, and been a good student. In all of my hours of studying and work, I have avoided failure...until now. Throughout this year, I have spent numerous hours in the lab following procedures to the best of my understanding and still failed over and over. Sometimes the issue was not my fault, but others it was. Experiencing failure was frustrating, but immensely more rewarding than I ever could have imagined. I have so much more appreciation for

33

Edison’s famous quote “I haven’t failed. I’ve just found 10,000 ways that won’t work<sup>24</sup>.” His view of failure is inspiring and serves as a great reminder that even when results do not turn out as hoped, there is something learned with each new attempt. Though this kind of learning may be unwanted, it can become even more valuable than any experimental result could ever be.

Seeing how even the smallest detail in an experiment can affect the entire outcome made me all the more grateful for the intricacies of God’s design. It is one thing to read about it and another to see it, meditate on it, and try to comprehend it in some small way. I have spent the past year and a half trying to understand this subject (on at

least some basic level) and found that the longer I study, the more I realize just how little I know and understand. Thinking back to the story of creation in at in all eight of the creative acts mentioned, God never lifts a finger. He simply *speaks*. Biblical scholar, Arthur Peake says, “By this effortless word God called the various orders of creation into existence...[there is] no struggle to bend the reluctant matter to His will, no laborious shaping and molding of raw stuff into the finished product, but the mere utterance of the word achieves at once and perfectly the divine intention<sup>25</sup>.” Creation was effortless for God, yet I could spend my entire life studying a single part of creation and never scratch the surface of understanding. That is God. Yet in His awe-inspiring power, He sees and knows and loves *us*.

Finally, maintaining this paradigm throughout this final semester brought about much needed perseverance. There were days when it was hard to go to the lab and work because the lack of results was immensely discouraging, but the book of James gives this assurance: “Blessed in the one who perseveres under trial because, having stood the test,

34

that person will receive the crown of life that the Lord has promised to those who love Him.” Though this may not be the greatest trial, God has still been faithful. This experience has been a “crown of life” in ways I never expected. It has caused me not only to better understand the scientific process, but also instilled in me an appreciation of creation and an awe of God’s power. Moreover, if He has proven faithful even in this small trial, His faithfulness will prove to be that much greater in a larger one. This is by far the most important result. *Soli Deo Gloria*.



B

35

## ibliography

1. "2017 Alzheimer's Disease Facts and Figures." *Alzheimer's & Dementia* 13 (2017): 325-73. *Alz.org*. Alzheimer's Association, 2017. Web. 12 April. 2017. 2.

"2015 Alzheimer's Disease Facts and Figures." *Alzheimer's & Dementia* 11.3 (2015): 332-84. *Alz.org*. Alzheimer's Association, 2015. Web. 19 Feb. 2016.

36

3. "Deaths and Mortality." *Centers for Disease Control and Prevention*. Centers for Disease Control and Prevention, 17 Mar. 2017. Web. 15 Apr. 2017. 4. "Alzheimer's Statistics." *Alzheimers.net*. A Place for Mom, Inc., 2016. Web. 15 Apr. 2017.

5. Park, So-Young, and Adriana Ferreira. "The generation of a 17 kDa neurotoxic fragment: an alternative mechanism by which tau mediates  $\beta$ -amyloid-induced neurodegeneration." *The Journal of neuroscience* 25.22 (2005): 5365-5375.

6. "Alzheimer's Disease." *Stanford Health Care*. Stanford Medical Center, 13 July 2016. Web. 15 Apr. 2017.
7. Fernandez-Funez, Pedro, Lorena de Mena, and Diego E. Rincon-Limas. "Modeling the complex pathology of Alzheimer's disease in *Drosophila*." *Experimental neurology* 274 (2015): 58-71.
8. Alavi Naini, Seyedeh Maryam, and Nadia Soussi-Yanicostas. "Tau Hyperphosphorylation and Oxidative Stress, a Critical Vicious Circle in Neurodegenerative Tauopathies?." *Oxidative medicine and cellular longevity* (2015).
9. Kolarova, Michala, et al. "Structure and pathology of tau protein in Alzheimer disease." *International journal of Alzheimer's disease* 2012 (2012).
10. Gistelink, Marc, et al. "Drosophila models of tauopathies: what have we learned?." *International Journal of Alzheimer's Disease* 2012 (2012).
11. Reinecke, James B., et al. "Implicating Calpain In Tau-Mediated Toxicity In Vivo." *Plos ONE* 6.8 (2011): 1-9. *Academic Search Premier*. Web. 6 Apr. 2016.

12. St Johnston, Daniel. "The art and design of genetic screens: *Drosophila melanogaster*." *Nature reviews genetics* 3.3 (2002): 176-188.
13. del Valle Rodríguez, Alberto, Dominic Didiano, and Claude Desplan. "Power tools for gene expression and clonal analysis in *Drosophila*." *Nature methods* 9.1 (2012): 47-55.
14. Jackson, George R. "Guide to understanding *Drosophila* models of

neurodegenerative diseases." *PLoS Biol* 6.2 (2008): e53.

15. Iyer, Janani, et al. "Quantitative assessment of eye phenotypes for functional genetic studies using *Drosophila melanogaster*." *bioRxiv* (2016): 036368. 16. Geng, Junhua, et al. "The C-terminus of Tau protein plays an important role in its stability and toxicity." *Journal of Molecular Neuroscience* 55.1 (2015): 251-259. 17. Yeh, P.-A. ( 1 ), et al. "Drosophila Notal Bristle As A Novel Assessment Tool For Pathogenic Study Of Tau Toxicity And Screening Of Therapeutic Compounds." *Biochemical And Biophysical Research Communications* 391.1 (2010): 510-516. Scopus®. Web. 6 Apr. 2016.

18. Povellato, Giulia, et al. "Modification of the *Drosophila* model of in vivo Tau toxicity reveals protective phosphorylation by GSK3 $\beta$ ." *Biology open* (2013): BIO20136692.

19. Bischof, Johannes, et al. "An optimized transgenesis system for *Drosophila* using germ-line-specific  $\phi$ C31 integrases." *Proceedings of the National Academy of Sciences* 104.9 (2007): 3312-3317.

20.

21.

22.

23.

24.

25.

26.

- 27.
28. "PhiC31 Vector System Overview." System Biosciences, Inc., 2013. 29.
- Hedgepeth, Chester M., et al. "Activation of the Wnt signaling pathway: a molecular mechanism for lithium action." *Developmental biology* 185.1 (1997): 82-91.
30. Science, Carnegie. "The Drosophila Gateway™ Vector Collection." *Carnegie Science*. Department of Embryology, 2017 Web. 15 Apr. 2017.
31. Invitrogen. "pENTR™ Directional TOPO® Cloning Kits." 2012. 32. Sarett, L. H. "Research and Invention." *Proceedings of the National Academy of Sciences of the United States of America*, vol. 80, no. 14, 1983, pp. 4572–4574., [www.jstor.org/stable/14073](http://www.jstor.org/stable/14073).
33. Peake, Arthur Samuel, and Alexander James Grieve, eds. *A Commentary on the Bible*. T. Nelson & sons, 1920.